ChemComm

RSC Publishing

COMMUNICATION

View Article Online
View Journal | View Issue

Orientated anatase TiO_2 nanocrystal array thin films for self-cleaning coating†

Cite this: *Chem. Commun.*, 2013, **49**, 8958

Received 18th June 2013,
Accepted 1st August 2013

DOI: 10.1039/c3cc44547j

www.rsc.org/chemcomm

Zhao Zhao,[ab] Huaqiao Tan,[a] Haifeng Zhao,[a] Di Li,[a] Min Zheng,[a] Peng Du,[ab] Guoqiang Zhang,[ab] Dan Qu,[ab] Zaicheng Sun*[a] and Hongyou Fan*[cd]

We developed a simple method to synthesize TiO_2 nanowire arrays with nearly 100% exposed {001} facets. The coating exhibits good transparency. The thin films of TiO_2 nanowire arrays display a very good photocatalytic degradation of dye molecules and good durability. Based on the above features, the TiO_2 nanowire array coating is advantageous for self-cleaning coating.

Anatase TiO_2, as one of the most promising wide band gap semi-conductor materials, has become a topic of intensive study due to its important photocatalytic property and related applications in photo-catalysis, dye-sensitive solar cells, photochromic devices and gas sensing.[1–6] The photocatalytic property of anatase TiO_2 crystals significantly relies on the access of high-energy facets such as {001}. Thus, controlled synthesis of anatase TiO_2 with both exposure of a high-energy facet and high surface area is technologically very important. Since the successful preparation of anatase TiO_2 crystals with a high percentage of exposed {001} facets by Lu *et al.* in 2008,[7] various TiO_2 nanostructures with high reactive facet have been developed using F^- compounds as a capping group.[8–10] The photo-catalytic performance shows a significant improvement when the TiO_2 nanostructures possess this well-defined crystal facet. Despite these important efforts, previous work mainly focused on powder specimens. For applications such as self-cleaning windows, sensors, filters *etc.*, nanostructured TiO_2 thin films with orientated high reactive facets are preferentially desirable. Due to the highly crystalline nature, direct synthesis of continuous, orientated TiO_2 thin films is a grand challenge. One of the alternative means is to grow thin films of nanocrystals or nanowire arrays of TiO_2. For example, TiO_2 nanowire arrays were fabricated through AAO template[11] electrochemical anodic oxidation[12] and hydrothermal[13] methods. For AAO and electrochemical anode methods, extra thermal treatment is required to create the anatase phase, but with less control of the {001} orientation. Through the hydrothermal synthetic route, only a rutile phase TiO_2 array was obtained in most cases. Recently, TiO_2 films exposed with 100% {001} facets were synthesized *via* a hydrothermal route with fluorine as a capping group.[14,15] The final TiO_2 layer showed great photocatalytic activity. However, the hydrothermal growth and nucleation process led to large crystal particles and caused scattering problems, which limits its applications in the field of self-cleaning coating.

Recently, our group developed a fluorine free hydrothermal route to prepare mesoporous anatase TiO_2 microspheres, which expose {001} facets on the surface. H_2SO_4 was used as both a phase-inducer for formation of the anatase phase and a capping agent to promote oriented growth and formation of the {001} facet. The resulting microspheres exhibited enhanced adsorption and photocatalytic degradation of rhodamine B in comparison with that of commercial Degussa P25 TiO_2.[16] Herein, we extended this technology and successfully synthesized thin films of orientated anatase TiO_2 nanowire arrays with nearly 100% exposed {001} facets. The thin film array shows great transparency and high photo-catalytic activity.

To synthesize orientated TiO_2 arrays, we grew a layer of anatase TiO_2 seeds on FTO glass substrates followed by continuous growth in 2 mol L^{-1} H_2SO_4 aqueous solution that contained tetrabutyl titanate (TBT). After 6 hours, a layer of TiO_2 nanowire arrays was grown on the substrate. The SEM plan view of a TiO_2 nanowire array is shown in Fig. 1A. It clearly shows that the TiO_2 array is about 1 micron thick and has a square-shaped nanomosaic $\sim$100 nm in size (Fig. 1). The fringe spacing in high-resolution TEM images and FFT image (Fig. 1C, inset) is 0.24 nm, which indicates that the surface of anatase TiO_2 nanowire arrays is {001} facet. The X-ray diffraction pattern (XRD) pattern (Fig. 1D) shows a significantly enhanced (004) diffraction peak, which matched with the crystalline anatase phase of TiO_2 (JCPDS no. 21-1272).

[a] *State Key Laboratory of Luminescence and Applications, Changchun Institute of Optics, Fine Mechanics and Physics, Chinese Academy of Sciences, 3888 East Nanhu Road, Changchun, Jilin 130033, P. R. China. E-mail: sunzc@ciomp.ac.cn*
[b] *University of Chinese Academy of Sciences, Beijing, P. R. China*
[c] *The University of New Mexico/NSF Center for Micro-Engineered Materials, Department of Chemical and Nuclear Engineering, Albuquerque, New Mexico 87131, USA*
[d] *Sandia National Laboratories, Advanced Materials Lab, 1001 University Blvd. SE, Albuquerque, New Mexico 87106, USA. E-mail: hfan@sandia.gov*

† Electronic supplementary information (ESI) available: Experimental details and additional SEM, TEM and contact angle images. See DOI: 10.1039/c3cc44547j

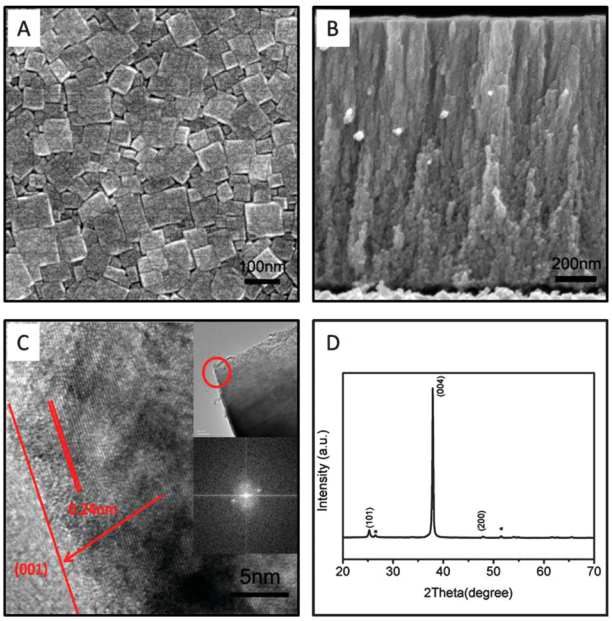

Fig. 1 Electron microscopy and XRD characterization of anatase TiO_2 nanowire array synthesized from 0.5 g TBT in 30 mL of 2.0 mol L^{-1} H_2SO_4 at 180 °C for 6 hours. (A) Field emission (FE) SEM images (plan view) of anatase TiO_2 nanowire array. (B) FE-SEM cross-sectional images of anatase TiO_2 nanowire array. (C) High-resolution TEM micrographs of mesoporous anatase TiO_2 micro-spheres. Top inset shows a piece of TiO_2 nanowire array. Bottom inset shows a fast Fourier transform micro-graph of the image area in C. (D) XRD patterns of anatase TiO_2 nanowire array on FTO glass.

To improve the transmission, PVP is added to the reaction to lower the thickness of the TiO_2 layer. The SEM plan view of TiO_2 nanowire arrays is shown in Fig. S1 (ESI†). It clearly shows that the film surface is composed of a nanomosaic ~20 nm in size. The thickness of the TiO_2 layer is ~440 nm when 1.0 g PVP was added to the reaction. The cross-sectional SEM image indicates that the TiO_2 layer consists of pearl-like long one-dimensional nanowires, which are normal to the surface. In comparison with the XRD pattern of FTO glass, the seed TiO_2 layer and TiO_2 nanowire array coated FTO glass (Fig. S1C, ESI†), the dramatic intensity enhancement of the (004) peak after growth on the FTO glass clearly indicates that the TiO_2 nanowires are oriented in the vertical direction and the film grows along the [001] direction. High resolution TEM proves that the surface of TiO_2 nanowire arrays is {001} facet.

Detailed studies indicated that the TiO_2 thin film nanostructure including thickness, transparency, and size of nanomosaic strongly depends on reaction conditions. We discovered that both the thickness of the film and the nanomosaic size on the film surface decrease with the increase of the PVP amount (Fig. S1 and S2, ESI†). The thickness of the TiO_2 nanowire array decreases from 1 micron to 500 nm, while the size of the nanomosaic changes to ~40 nm when 0.5 g PVP is added to the reaction. This is probably due to PVP binding which restrains further growth of TiO_2 crystals.[17] This strategy has been used previously to control crystal shape and size.[18,19] We also investigated the influence of reaction time on the TiO_2 nanostructure (Fig. 2). The {001} facet is developed at the very beginning stage (within 1 hour). Then nanomosaic becomes

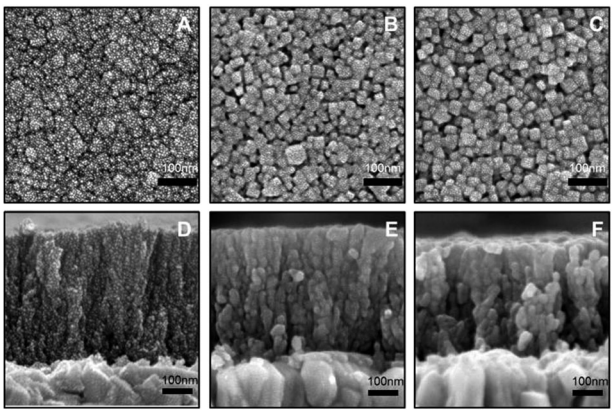

Fig. 2 FE-SEM images (plan view A–C and cross-sectional view D–F) of TiO_2 nanowire array obtained from 0.5 mL TBT and 1.0 g PVP in 30 mL of 2 mol L^{-1} H_2SO_4 solution at 180 °C for 1 h (A and D), 12 h (B and E), and 24 h (C and F).

more and more clear along the course of the reaction until the appearance of a square shape at ~6 hours. After that, the size of mosaic becomes bigger and more well-defined (Fig. 2A–C). The sharpness of the nanomosaic during growth is likely due to the acid etching during the reaction.[16] The etching step produces more pores from the surface toward the interior of the array. The cross-sectional specimens were prepared to evaluate the film thickness change with the reaction time (Fig. 2D–F). The result in Fig. 2D–F shows that the thickness does not change too much with the reaction time.

We evaluated the transparency with different film thicknesses. Fig. 3A shows the transmission of a bare FTO glass, thin films of TiO_2 nanowire arrays prepared in the absence and presence of PVP. The bare FTO shows ~80% transmission. In the case of the TiO_2 coating obtained in the absence of PVP, the transmission decreased about 10% when the film thickness was ~1 micron. When the film thickness decreases to ~440 nm (prepared in the presence of PVP), the film shows the same transparency as the bare FTO glass. We also studied the durability of the nanowire films. All the films we prepared passed the type test which indicates that the nanowire arrays have good adhesion on FTO substrates.

The wettability of the surface is a key parameter for self-cleaning coating. Fig. 3B shows the contact angle of the TiO_2

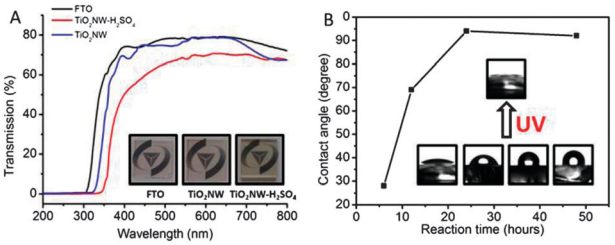

Fig. 3 (A) Transparency of a FTO substrate and thin films of TiO_2 nanowire array prepared in the absence (TiO_2 NW–H_2SO_4, red) and presence (TiO_2 NW, blue) of PVP. Insets are corresponding optical pictures. (B) Contact angle of TiO_2 nanowire array obtained from 0.5 mL TBT and 1.0 g PVP in 2 mol L^{-1} H_2SO_4 solution for different reaction times. Insets are contact angle optical images from left to right, 6, 12, 24 and 48 hours; top image is a typical contact angle image of the sample after UV treatment.

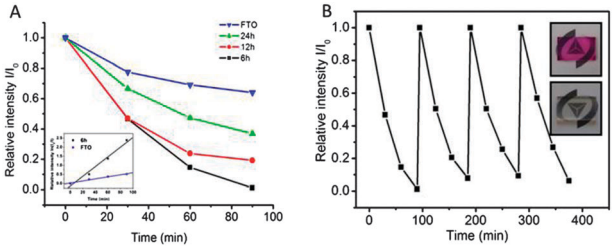

Fig. 4 Comparison of photocatalytic degradation rates of rhodamine B on FTO glass and TiO_2 nanowire array synthesized in 0.5 g TBT and 1.0 g PVP in 30 mL of 2 mol L^{-1} H_2SO_4 solution at 180 °C for 6, 12, and 24 hours. (B) Cycling degradation curve of TiO_2 nanowire array on FTO glass.

film on the FTO substrate for different reaction times. It clearly shows that the contact angle increases from 28° to 90° for 6 to 48 hours reaction time. The possible reason is that the longer time the reaction proceeds, the more porous is the surface of the film due to the acid-etching process.[14] The porous surface may trap more air leading to higher contact angles. When the TiO_2 nanowire film was treated with UV light, the contact angle rapidly decreased to ~6° in all cases (Fig. 3B inset and Fig. S3, ESI†), which means the surface of TiO_2 nanowire arrays turned super hydrophilic.

We studied the photocatalytic property of resulting TiO_2 nanowire thin films. The photocatalytic activities of the TiO_2 nanowire array coating obtained at different degradation times were evaluated by monitoring the decomposition of Rhodamine B (RhB) on the surface of FTO glass and TiO_2 nanowire array under UV irradiation. RhB was deposited on the TiO_2 films through spin-coating using a 0.5 mg mL^{-1} RhB solution at 1000 rpm for 1 min. It showed a purple color at the initial point as shown in Fig. 4B (inset). After UV irradiation for 90 min, the glass turned fully transparent, which indicated that RhB was decomposed under UV irradiation. The kinetics of RhB degradation is presented in Fig. 4A. I is the absorption intensity of RhB after UV irradiation for a certain period, and I_0 is the absorption of RhB at the initial point. After irradiation for 90 min, nearly 95% of RhB is degraded by the TiO_2 nanowire array coating prepared for 6 hours, whereas other samples including FTO glass and TiO_2 nanowire arrays synthesized for 24 and 12 hours exhibit lower activities with degradation rates of about 36%, 64%, and 81%, respectively. The rate of photocatalytic degradation of RhB shows a linear profile. The rate of photocatalytic degradation is 0.005 and 0.027 for FTO glass and TiO_2 nanowire arrays obtained from 6 hours, respectively. FTO showed some degree of degradation because SnO_2 is a semiconductor. With TiO_2 nanowire arrays, photocatalytic capability is significantly enhanced, because the exposed surface is a high reactive {001} facet of TiO_2 nanocrystals. Fig. 4B displays the durability of TiO_2 nanowire arrays for photocatalytic degradation of RhB under UV irradiation. After the recycled experiments, the photocatalytic activity remains unchanged.

In summary, we developed a simple method to synthesize TiO_2 nanowire arrays with nearly 100% exposed {001} facets. The coating exhibits good transparency. The thin films of TiO_2 nanowire arrays display a very good photocatalytic degradation of dye molecules and good durability. Based on the above advantages, this TiO_2 nanowire array coating is potentially used for self-cleaning coating.

Notes and references

1 X. Chen and S. S. Mao, *Chem. Rev.*, 2007, **107**, 2891–2959.
2 M. Graetzel, R. A. J. Janssen, D. B. Mitzi and E. H. Sargent, *Nature*, 2012, **488**, 304–312.
3 M. A. Henderson, *Surf. Sci. Rep.*, 2011, **66**, 185–297.
4 Y. Li, T. Sasaki, Y. Shimizu and N. Koshizaki, *Small*, 2008, **4**, 2286–2291.
5 Y. Li, T. Sasaki, Y. Shimizu and N. Koshizaki, *J. Am. Chem. Soc.*, 2008, **130**, 14755–14762.
6 R. Wang, K. Hashimoto, A. Fujishima, M. Chikuni, E. Kojima, A. Kitamura, M. Shimohigoshi and T. Watanabe, *Nature*, 1997, **388**, 431–432.
7 H. G. Yang, C. H. Sun, S. Z. Qiao, J. Zou, G. Liu, S. C. Smith, H. M. Cheng and G. Q. Lu, *Nature*, 2008, **453**, 638–641.
8 J. Pan, G. Liu, G. Q. Lu and H.-M. Cheng, *Angew. Chem., Int. Ed.*, 2011, **50**, 2133–2137.
9 X. Zhao, W. Jin, J. Cai, J. Ye, Z. Li, Y. Ma, J. Xie and L. Qi, *Adv. Funct. Mater.*, 2011, **21**, 3554–3563.
10 L. Bao, Z.-L. Zhang, Z.-Q. Tian, L. Zhang, C. Liu, Y. Lin, B. Qi and D.-W. Pang, *Adv. Mater.*, 2011, **23**, 5801–5806.
11 Z. Miao, D. Xu, J. Ouyang, G. Guo, X. Zhao and Y. Tang, *Nano Lett.*, 2002, **2**, 717–720.
12 G. K. Mor, K. Shankar, M. Paulose, O. K. Varghese and C. A. Grimes, *Nano Lett.*, 2005, **6**, 215–218.
13 B. Liu and E. S. Aydil, *J. Am. Chem. Soc.*, 2009, **131**, 3985–3990.
14 R. Liu, D. Wu, X. Feng and K. Müllen, *J. Am. Chem. Soc.*, 2011, **133**, 15221–15223.
15 A. S. Ichimura, B. M. Mack, S. M. Usmani and D. G. Mars, *Chem. Mater.*, 2012, **24**, 2324–2329.
16 Z. Zhao, Z. Sun, H. Zhao, M. Zheng, P. Du, J. Zhao and H. Fan, *J. Mater. Chem.*, 2012, **22**, 21965.
17 P. Wang, D. Wang, H. Li, T. Xie, H. Wang and Z. Du, *J. Colloid Interface Sci.*, 2007, **314**, 337–340.
18 B. Wiley, T. Herricks, Y. Sun and Y. Xia, *Nano Lett.*, 2004, **4**, 1733–1739.
19 S. H. Im, Y. T. Lee, B. Wiley and Y. Xia, *Angew. Chem., Int. Ed.*, 2005, **44**, 2154–2157.

